FERMILAB-PUB-23-411-AD-PPD-SQMS-TD

Prepared for submission to JINST

Superconducting radio frequency linear collider HELEN

S. Belomestnykh,[a,b,1] **P.C. Bhat,**[a] **A. Grassellino,**[a] **M. Checchin,**[c] **D. Denisov,**[d] **R.L. Geng,**[e] **S. Jindariani,**[a] **M. Liepe,**[f] **M. Martinello,**[c] **P. Merkel,**[a] **S. Nagaitsev,**[e] **H. Padamsee,**[a,f] **S. Posen,**[a] **R.A. Rimmer,**[e] **A. Romanenko,**[a] **V. Shiltsev,**[a] **A. Valishev,**[a] **V. Yakovlev**[a]

[a] *Fermi National Accelerator Laboratory, Batavia, IL, USA*

[b] *Stony Brook University, Stony Brook, NY, USA*

[c] *SLAC National Accelerator Laboratory, Menlo Park, ca, USA*

[d] *Brookhaven National Laboratory, Upton, NY, USA*

[e] *Thomas Jefferson National Accelerator Facility, Newport News, VA, USA*

[f] *Cornell University, Ithaca, NY, USA*

E-mail: sbelomes@fnal.gov

Abstract: This article discusses a proposed Higgs-Energy LEptoN (HELEN) e^+e^- linear collider based on advanced traveling wave superconducting radio frequency technology. The proposed collider offers cost and AC power savings, smaller footprint (relative to the ILC), and could be built at Fermilab. After the initial physics run at 250 GeV, the collider could be upgraded either to higher luminosity or to higher, up to 500 GeV, energies.

Keywords: Particle Colliders, Superconducting RF, Accelerator Subsystems and Technologies

[1] Corresponding author.

Contents

1 Introduction

Since the discovery of the Higgs boson in 2012, there is great interest in the world's collider physics community in an e^+e^- collider operating at $\sqrt{s}$ = 250 GeV (Higgs factory) and above, to make precision measurements of the Higgs boson couplings and searches for physics beyond the Standard Model. For many years, the International Linear Collider (ILC) based on superconducting radio frequency (SRF) accelerator technology has been a forerunner proposal for such a machine. Its mature SRF technology has been "shovel ready" and has been used to build such SRF linacs as European XFEL in Hamburg, Germany, and LCLS-II / LCLS-II-HE at SLAC in the USA.

In the meantime, SRF researchers around the world continued to make progress in developing SRF cavities with higher accelerating gradients and quality factors. The accelerating gradients up to 50 MV/m were demonstrated in TESLA shape (ILC) cavities, significantly higher than the ILC design specification of 31.5 MV/m. On the other hand, a traveling wave SRF structure with a feedback waveguide has lower surface electromagnetic fields than standing wave cavity geometries, thus promising higher accelerating gradients for the same surface fields. It is expected that with an aggressive R&D program on traveling wave SRF structures and innovations in cavity surface

treatments and processing, an accelerating gradient of about 70 MV/m can possibly be reached within the next few years.

Anticipating these advances in the near future, we proposed a more compact and cost-effective SRF-based e^+e^- linear collider, named Higgs-Energy LEptoN (HELEN) collider, that can be sited at Fermilab [1]. In this paper we briefly review the physics at Higgs factory first. As at the core of HELEN collider is the SRF technology, we then discuss current limitations of the SRF technology for ILC followed by a brief review of relevant advances in SRF beyond the state of the art. The HELEN collider is described in some details including tentative list of parameters, layout and possible siting, and potentials for luminosity and energy upgrades. Following that we discuss approaches to a detector for this collider. The last section is dedicated to an outline of the accelerator and detector R&D objectives. Finally, we provide brief summary and conclusions.

2 Physics at Higgs factory

Here we provide general statements about physics at the e^+e^- Higgs factories. Detailed physics studies for the e^+e^- colliders have been conducted by the ILC, FCC, CLIC, and CEPC collaborations [2–5]. Physics reach of HELEN should be similar to ILC, assuming that the same integrated luminosity and beam polarization levels are achievable.

The Standard Model (SM) of elementary particles has been validated extensively through precision experiments and found to be incredibly successful at describing our world. However, despite being internally consistent and very successful, there are a number of experimental observations that the SM fails to explain. It does not fully explain the baryon asymmetry, incorporate the theory of gravitation as described by general relativity, or account for the accelerating expansion of the Universe as possibly described by dark energy. The model does not contain any viable dark matter particle that possesses all of the required properties deduced from cosmology and astrophysics. It also does not incorporate neutrino oscillations and their non-zero masses. Furthermore, the model suffers from several internal shortcomings, such as the hierarchy problem, where fine-tuned cancellations of large quantum corrections are required in order for the Higgs boson mass to be near the electroweak scale. It is evident that the Standard Model is just an effective theory that appears, so far, to be valid at the energies experimentally accessible today.

For the next two decades, the LHC will remain the highest energy collider in the world. The full LHC dataset is expected to be 20 times more than what we have today. Such a dataset will provide great opportunities for studies of the SM, including detailed characterization of the Higgs boson. Besides the precision, the LHC data will also greatly extend the sensitivity for new physics. However, it is conceivable that the HL-LHC dataset will not be sufficient to discover and fully characterize new physics. This provides a strong motivation for an e^+e^- Higgs factory.

Detailed exploration of the electroweak sector of the Standard Model remains a high priority. An e^+e^- Higgs factory will enable highly precise measurements of Standard Model parameters, which in turn provide deeper insight into the mechanism of electroweak symmetry breaking. This includes precise determination of the nature of the Higgs boson, including measurements of its properties and couplings. It has been demonstrated that a wide range of new physics models with multi-TeV scale result in few percent level modifications to the Higgs boson couplings [6]. Therefore, measuring Higgs boson couplings at the sub-percent level can provide first indirect

evidence of beyond-SM (BSM) particles or forces. Measurements of the Higgs boson decay rate to invisible particles is also very important for discovering or constraining BSM physics. Beyond the couplings, measurement of the Higgs boson total width and self-interactions (both trilinear and quartic) would further shed light on the underlying structure of the electroweak sector; these measurements (as well as top Yukawa coupling) however require e^+e^- collision energies of 500 GeV or higher.

While the Higgs boson remains a centerpiece for the precision program at Higgs factories, many other rare SM processes continue to attract significant interest. For example, operation at lower energies on the Z resonance (91 GeV) and at the WW threshold (160 GeV) will allow to gather large amounts of data and perform precision measurements of the electroweak sector of the SM. An e^+e^- collider with luminosity of 10^{34} cm^{-2}s^{-1} will produce billions of Z boson and tens of millions of WW events. This dataset will allow to significantly improve current precision of the key electroweak observables, such as the weak mixing angle ($\sin^2(\theta_{\rm eff})$), the masses and widths of the W and Z bosons, the forward-backward asymmetry for bottom quarks (A_b) and the polarization asymmetry of tau leptons (A_τ). A very precise determination of the strong coupling constant α_s at the M_Z scale and the number of weakly-interacting neutrinos are also possible.

Besides the precision, e^+e^- colliders offer excellent opportunities for direct observation of new physics, covering many orders of magnitude of coupling strengths and mass scales. For example, signatures of dark photons and axion-like particles can be searched for in decays of the Z bosons produced in the 91 GeV run. New resonances (Z') with masses up to the collision energy and decaying into fermion (f) pairs, predicted by many extensions to the SM (e.g., compositeness, extra dimensions, etc.), can be discovered in the $e^+e^- \to ff$ process. In SUSY, low momentum thresholds available at the e^+e^- colliders enable excellent capability to look for naturally light and compressed electroweakino states that are very challenging at the hadron machines, thus providing a nice complementarity to the LHC searches. Finally, a wide class of BSM models with extended Higgs sectors can be probed by looking for pair production of the additional Higgs bosons.

It is evident from the considerations above that HELEN collider opens window to a rich and exciting physics program, with excellent chances for fundamental discoveries.

3 SRF technology for linear colliders

3.1 SRF for ILC: state of the art and limitations

Superconducting radio frequency technology for a linear collider has been in development since early 1990's [7]. The SRF option was selected for the International Linear Collider (ILC), which has been the prime candidate for a next lepton HEP collider, especially since the discovery of the Higgs boson in 2012. The machine was baselined in 2013 [8, 9] and is under consideration to be hosted in Japan. The collider facility will be about 20.5 kilometers in total length, and will accelerate beams of electrons and positrons to 125 GeV each to operate at the center-of-mass energy of 250 GeV, see e.g., [10]. The design instantaneous luminosity of the collider will be 1.35×10^{34} cm^{-2}s^{-1} with proposals to upgrade to higher luminosity (up to 8.1×10^{34} cm^{-2}s^{-1} or, accounting for polarization, with an effective luminosity up to 2.0×10^{35} cm^{-2}s^{-1}) [11].

The baseline ILC SRF technology is well-established [12] and has already been used to build such machines as European XFEL [13] and LCLS-II [14]. The ILC design specifies an accelerating

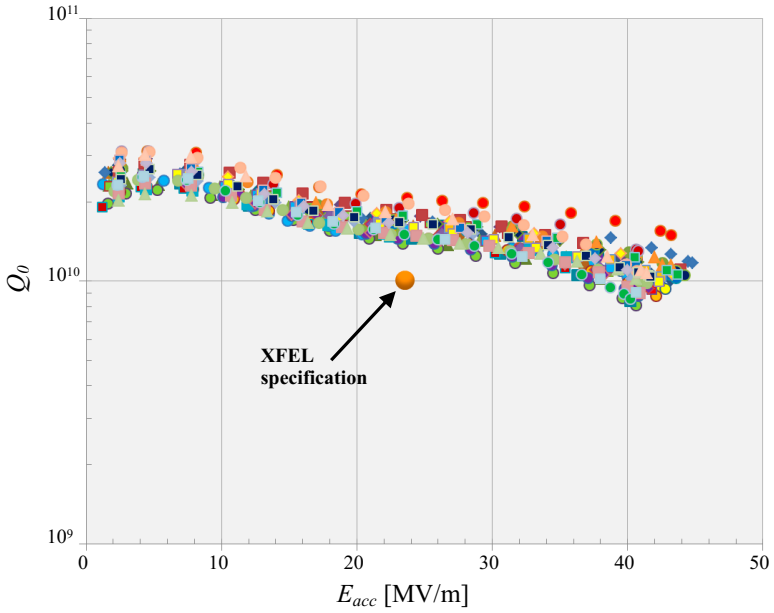

Figure 1. Performance of 47 best cavities from the European XFEL production run.

gradient E_{acc} of 31.5 MV/m and intrinsic cavity quality factor Q of 1×10^{10} per the ILC Technical Design Report (TDR) [8, 9]. During phase II of the ILC R&D program, the (94 ± 6)% yield has been achieved for cavities that demonstrated accelerating gradients >28 MV/m and (75 ± 11)% for 35 MV/m. These yields were reached after cavities with gradients outside the ILC specification have been re-treated. This ensemble of cavities has an average gradient of 37.1 MV/m. At DESY, two large-grain 9-cell cavities also reached 45 MV/m [15].

The performance of European XFEL cavities is close to the requirements of the ILC TDR. The 420 cavities from one vendor which followed the ILC electropolishing (EP) recipe for final treatment succeeded in reaching an average gradient of 33.0 ± 6.5 MV/m. More than 10% of cavities from this vendor exceeded 40 MV/m. Figure 1 shows performance plots for 47 "best" cavities from the European XFEL production run, all reaching accelerating gradient in the 40–45 MV/m range [16]. The average cryomodule gradient reached was 27.5 ± 4.8 MV/m. So, the cryomodule performance does need to be improved to reach ILC specs of 31.5 MV/m. However, it is very encouraging that 18 out of 97 cryomodules reached the operating gradient of > 30 MV/m, which is close to the ILC-TDR specification. About 50% of all cavities tested in 97 modules have operating gradients above or equal to the 31 MV/m administrative limit [17]. Since the start of operation in 2017, the accelerator has demonstrated remarkable reliability and availability. In 2022 the machine availability during 4200 hours of X-Ray Delivery was approximately 96.6% excluding cryogenic system cold compressor failures. Over the last 5 years, an average of only 1 cavity per year has been detuned due to activation of a field emitter [18]. The demonstrated success from the European XFEL cavity and cryomodule production is a very good indication that the ILC goals are within reach. It is rare that an approximately 10% prototype demonstration exists for a new HEP machine, and for its core technology.

Two laboratories have continued efforts to demonstrate the ILC cryomodule (CM) goal, but on a smaller scale. An ILC demonstration cryomodule prepared by Fermilab reached the total available accelerating voltage of 267.9 MV, which is equivalent to an average gradient of 32.2 MV/m for eight cavities, thus exceeding the ILC goal. A beam with the 3.2 nC bunch charge has obtained an energy gain of >255 MeV after passing through the CM [19]. Nine (including one nitrogen-infused cavity) out of twelve cavities in a demonstration cryomodule at the KEK test facility (STF) exceeded the ILC specification, achieving an average accelerating gradient of 33 MV/m during beam operation [20]. Three of these cavities exceeded 36 MV/m. Cavities for a new high gradient demonstration module at Fermilab have reached 40 MV/m average in their vertical tests. The CM test with these cavities has yet to be conducted.

One can claim that the SRF technology for ILC at 250 GeV is "shovel-ready". The technology has been demonstrated and industrialized. Besides European XFEL, new large scale facilities – LCLS-II / LCLS-II-HE, ESS, PIP-II, and SHINE – are soon to be commissioned or under construction. Extensive SRF infrastructure exists worldwide for cavity fabrication, surface treatment, clean assembly, cold testing, and cryomodule assembly. Major SRF facilities are available at DESY, CERN, INFN, CEA/Saclay, IJCLab, KEK, JLAB, Cornell, Fermilab, MSU, and at several industries around the world. New infrastructure is becoming available for upcoming projects such as ESS in Europe, and PAPS in China. New industries in South Korea, China, and Japan are rapidly growing familiar with SRF technology.

It is expected that the SRF gradient and Q technology to continue to advance, reaching 40 MV/m at Q's of 2×10^{10}. R&D needs to be carried out to bring these results from single cell to 9-cell cavities. With an investment of $\sim$ 1.5 B ILCU for new cryomodules housing about 3,000 cavities and additional conventional construction, the ILC will be upgradeable to higher collision energies up to 380 GeV in the future, as out lined in [11]. In principle, upgrades to 500 GeV, 1 TeV, and beyond are possible [10, 21].

3.2 SRF technology advances beyond ILC

3.2.1 Advances in surface preparation of standing wave SRF cavities

Superconducting RF technology continues to move forward. In this section, we describe the ongoing R&D program to improve the gradient and Q of SRF accelerating structures made of bulk niobium via new surface preparation techniques. Application of these newly developed techniques to travelling wave structures with lower peak fields than those of standing wave structures will open the door to 70 MV/m superconducting RF for HELEN, as will be described in section 3.2.2.

Key area of development over the last 5–10 years have been for higher Q values at medium gradients (16–25 MV/m) for CW operation with the invention of new techniques of nitrogen doping (N-doping) [22]. A remarkable outcome of N-doping is the rise in Q with field, as opposed to standard fall in Q behavior with the ILC cavity surface treatment. Nitrogen doping for high Q has already been applied to the construction of LCLS-II, and its high energy upgrade LCLS-II-HE. For LCLS-II, more than 300 1.3-GHz cavities in 38 cryomodules have been delivered to SLAC, and 35 are installed in the tunnel (the other 3 are spares). For LCLS-II-HE, ten 1.3 GHz 9-cell N-doped cavities have reached average gradient of 25.9 MV/m and average Q of 3.6×10^{10} at 23 MV/m (the acceptance gradient for vertical cavity tests) (Figure 2) [23].

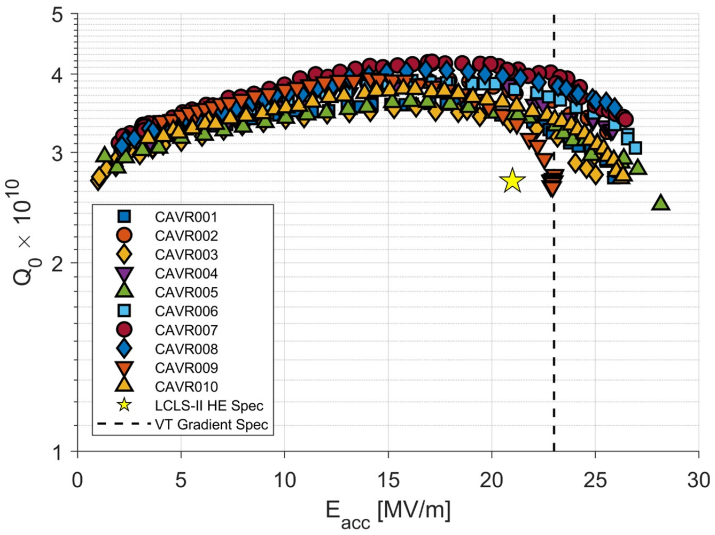

Figure 2. Q vs. E_{acc} curves for ten LCLS-II-HE 9-cell cavities processed with 2/0 N-doping recipe followed by cold EP [23].

Further Q improvements come from exciting developments [24] that show $Q = 5 \times 10^{10}$ at 30 MV/m by baking at $\sim$ 300°C (medium-temperature, or mid–T, baking) to dissolve the natural oxide and other surface layers into the bulk. It is interesting to note (Figure 3) how the Q rises with field, as seen for N-doping. After exposure to air, followed by High-Pressure Rinsing with ultra-pure deionized water (HPR), the Q dropped to 2×10^{10} at 30 MV/m. Surface analysis of similarly treated samples show a nitrogen peak at a few nm below the surface, suggesting that nitrogen is naturally present at the surface and has diffused into the Nb to give the N-doping effect. IHEP in Beijing, China followed up on these encouraging results with similar exciting results on several 9-cell TESLA cavities [25]. After mid–T (300°C) furnace bake, and HPR, all the 9-cell cavities demonstrate high Q in the range of $3.5 - 4.4 \times 10^{10}$ at the gradient between 16 and 24 MV/m, as shown in Figure 4. KEK is also pursuing the mid–T baking option. Although in its early stages, the mid–T baking procedure shows the potential of Nb for high gradients with high Q's.

On the high gradient frontier (with higher Q's), the invention of nitrogen infusion [26] (N-infusion, stemming from the discovery of nitrogen doping) demonstrated gradients of 40–45 MV/m as shown in Figure 5, and compared to the lower performance of cavities prepared with the standard ILC recipe. In yet another new and extraordinary development at FNAL, quench fields near 50 MV/m for 1.3 GHz TESLA-shaped SRF single-cell cavities have been achieved with a new 75/120°C two-step bake treatment followed by cold EP [27], as shown in Figure 6(a). This surface treatment shows gradients in the range of 40–50 MV/m (average 45 MV/m), as depicted by the histogram of about 50 tests in Figure 6(b) [28]. Note that 3 cavities that quench below 28 MV/m were found to have rare physical defects that likely limited their performance.

3.2.2 Nb-based traveling wave SRF

Since the peak surface magnetic field H_{pk} presents a hard ultimate limit to the performance of Nb cavities via the critical superheating field, it is beneficial to develop new geometries to improve

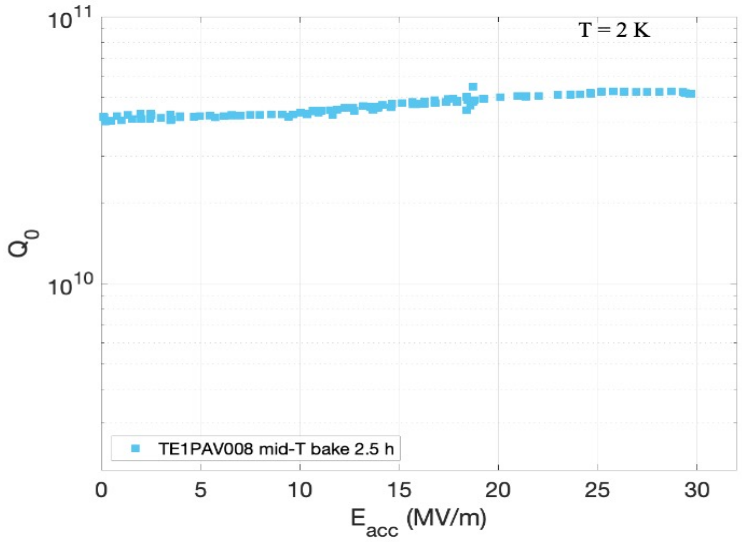

Figure 3. $Q = 5 \times 10^{10}$ at 30 MV/m by baking at ~ 300°C to dissolve the natural oxide (and other surface layers) into the bulk, but not exposing the cavity to air or water before RF measurements.

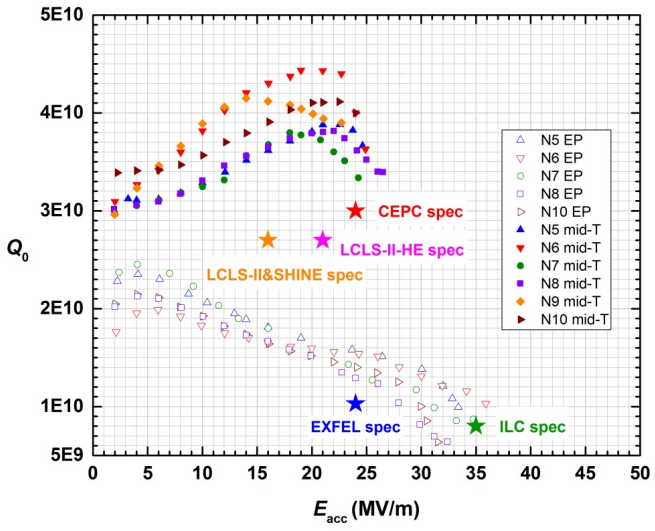

Figure 4. Results from IHEP (China) on mid–*T* baking 9-cell cavities after exposure to air and high pressure water rinsing. The results are compared to those with the standard ILC treatment.

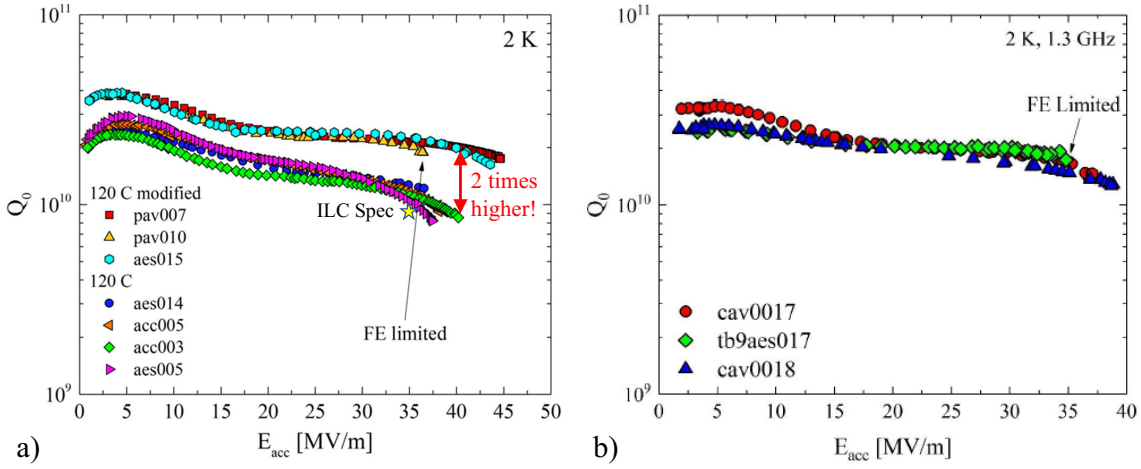

Figure 5. Nitrogen infusion results: (a) single-cell cavities, (b) 9-cell cavities.

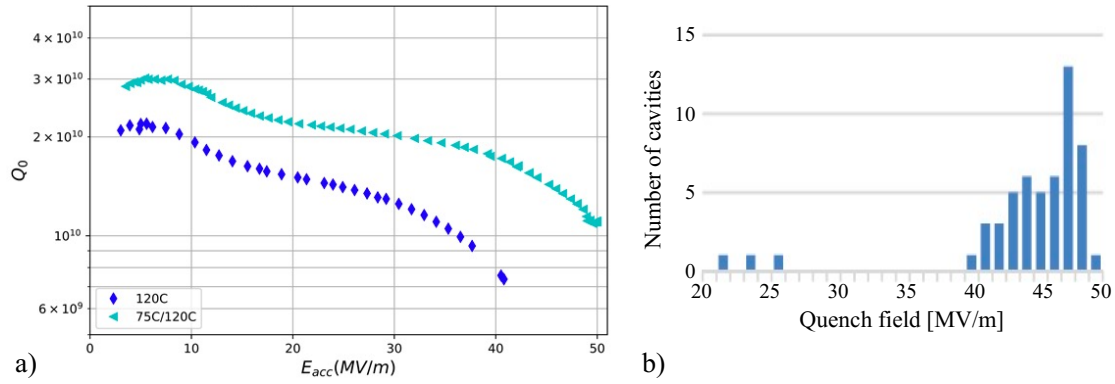

Figure 6. (a) Q vs. E curve of single-cell cavity reaching 49 MV/m from cold EP / optimized baking (75/120°C) compared to the curve of a cavity prepared by the standard ILC recipe. (b) Histogram of gradients of a large number of single-cell cavities prepared by cold EP / optimized baking (75/120°C).

upon the standing wave TESLA cavity geometry. As we have seen earlier, the newly developed, two-step baking procedure has demonstrated gradients up to ~ 50 MV/m in TESLA shape single-cell cavities. Combining the two-step bake with the advanced shape cavities has the potential of significantly improving the accelerating gradients.

One of the promising SRF structures is an SRF cavity operating in a traveling wave (TW) regime. Operation of superconducting RF structures in traveling wave regime was first studied in mid-1960s with a detail analysis published by Neal in 1968 [29]. As attenuation of the SRF structure is extremely low, one must avoid wasting electromagnetic power at the end of the structure. This is done by implementing a resonant ring set up, in which the residual RF power at the end of the accelerating cavity is fed back to the input end via a waveguide, where it is combined with the source power and fed back to the accelerator, as shown in Figure 7.

RF power can be coupled to the feedback waveguide in several different ways: via an RF bridge

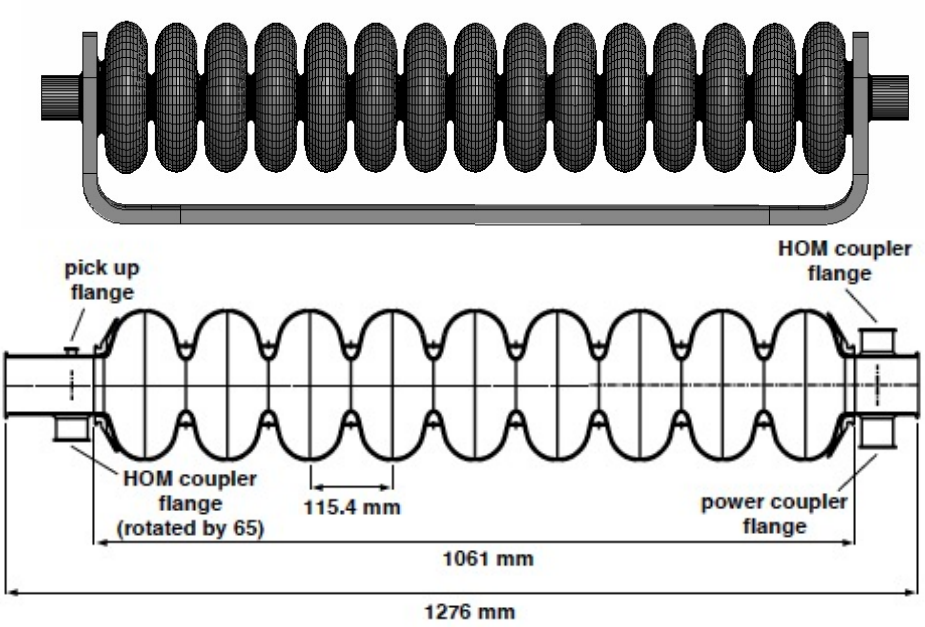

Figure 7. The TW structure with a 105° phase advance per cell compared to the one-meter standing-wave TESLA structure [12].

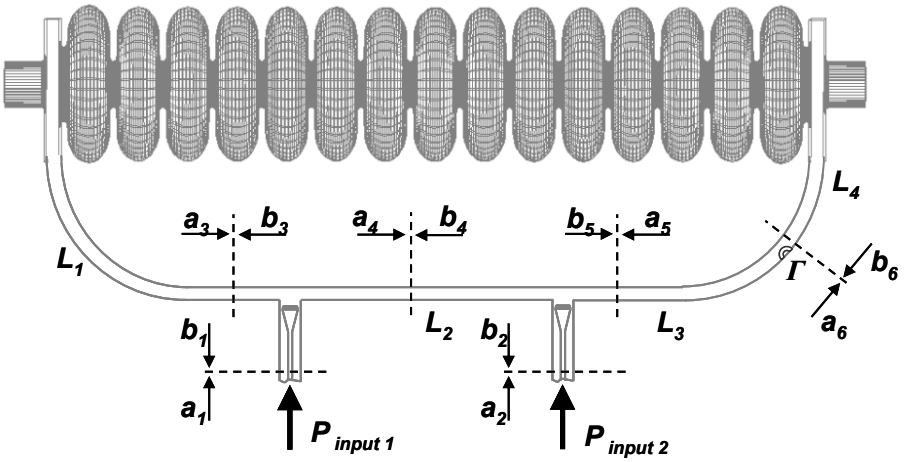

Figure 8. Two-coupler scheme for excitation of the TW resonant ring [30].

(as was proposed originally in [29]) or either one- or two-RF-coupler schemes [30]. Figure 8 shows a schematic of the 2-coupler scheme. Forward traveling wave can be excited inside the resonant ring by carefully selecting RF power distribution and phase difference between the two input signals. An adjustable "matcher" with reflection coefficient Γ is used to cancel reflection and thus suppress the unwanted backward wave. The matcher in combination with a conventional frequency tuner will be utilized by a resonant control feedback loop. Dashed lines indicate boundaries of the waveguide sections for scattering matrix analysis of the system. Vectors a_i and b_i indicate the incident and reverse waves at the boundaries. L_i is the section length.

Travelling wave structures offer several advantages compared to standing wave structures. Substantially lower (H_{pk}/E_{acc}) and lower (E_{pk}/E_{acc}) ratios of peak magnetic and peak electric fields to the accelerating gradient promise achieving higher E_{acc} at the same magnetic quench limit. Approximately a factor of 2 higher R/Q would ensure lower cryogenic losses. In addition, the TW structure provides high stability of the field distribution along the structure with respect to geometrical perturbations. This allows for much longer accelerating structures than TESLA cavities, limited by the manufacturing technology only.

The emphasis of the design optimization should be to lower H_{pk}/E_{acc}, as much as possible, since H_{pk} presents a hard ultimate limit to the performance of Nb cavities via the critical superheating field. But, as Figure 7 shows, the TW structure requires almost twice the number of cells per meter as for the SW structure in order to provide the proper RF phase advance (about 105 degrees), as well as a feedback waveguide for redirecting power from the end to the front of the accelerating structure, which avoids high peak surface fields in the accelerating cells. The feedback waveguide requires careful tuning to compensate reflections along the TW ring and thus obtain a pure traveling wave regime at the desired frequency.

Table 1 [31] shows one set of parameters for optimized cell shape, RF phase advance, and 50 mm aperture that yield H_{pk}/E_{acc} = 28.8 Oe/(MV/m) with E_{pk}/E_{acc} = 1.73. The geometrical parameters for the cell shape are defined in Figure 9. A smaller aperture than the 70 mm one of the TESLA cavity allows significant increase of accelerating gradient because of smaller H_{pk}/E_{acc} for the same E_{pk}/E_{acc}. The reduced 50 mm aperture should not cause any major issues in the TW structure due to high cell-to-cell coupling. In contrast, such aperture in a SW structure would likely introduce trapped modes due to weak cell-to-cell coupling. Since H_{pk}/E_{acc} is 42.6 Oe/(MV/m) for the TESLA structure, the TW structure has reduced the critical parameter H_{pk}/E_{acc} by a factor of 1.48! If results for the best single cell TESLA shape cavities prepared today (E_{acc} = 49 MV/m, H_{pk} = 2090 Oe) can be reached in such a TW structure, we can optimistically expect a gradient $E_{acc} > 70$ MV/m.

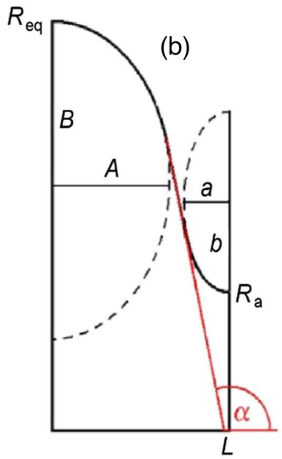

Figure 9. Geometry of the TW half cell.

The 100% R/Q increase (even with somewhat lower G of 186 Ohm vs. 270 Ohm for TESLA) lowers the dynamic heat load and cryogenic power needed for high gradients. Studies [31] show

Optimization	120/200
Phase advance (deg.)	90
A (mm)	23.83
B (mm)	36.40
a (mm)	4.51
b (mm)	7.52
E_{pk}/E_{acc}	1.727
B_{pk}/E_{acc} (mT/(MV/m))	2.878
R_{sh}/Q (Ohm/m)	2,127
α (deg.)	90.91
R_{eq} (mm)	98.95
v_{gr}/c	0.01831
E_{acc} (MV/m)	69.5
$E_{acc} \cdot 2L$ MV	4.00

Table 1. Parameters of optimized cells with limiting surface fields E_{pk} = 120 MV/m and B_{pk} = 200 mT; $L - A$ = 5 mm, aperture radius R_a = 25 mm (from [31], Table III, column 3.) Geometrical parameters are shown in Figure 9.

that the cell shape can be fine-tuned to avoid multipacting, without increasing H_{pk} more than 1%. Higher Order Mode (HOM) damping for TW structures is under study. Preliminary results demonstrate that the first 10 monopole modes up to 7 GHz show no trapping.

The high group velocity in the TW mode also increases the cell-to-cell coupling, which in turn relaxes manufacturing tolerances or allows to make longer structures while maintaining the same field errors as in TESLA cavities. The coupling coefficient k_{TW} of the TW structure is related to the group velocity as

$$k_{TW} = 2\beta_{gr}/(\theta \sin\theta)\,, \tag{3.1}$$

where θ is the RF phase advance per cell, $\beta_{gr} = v_{gr}/c$ is the group velocity relative to light. For $\beta_{gr} = 0.01831$ (Table 1) and $\theta = 90°$ we have $k_{TW} = 2.34 \times 10^{-2}$. We know that the SW π-mode TESLA structure with $k_{SW} = 1.8 \times 10^{-2}$ can be tuned. To maintain the same field errors, we can increase the number of cells in the TW structure up to

$$N_{TW} = 2\,(k_{TW}/k_{SW})\,N_{SW}^2. \tag{3.2}$$

The length of this structure will be $L_s = N_{TW} L_c$, where $L_c = \lambda\theta/(2\pi)$ is the cell length. Thus, we get

$$L_s = \frac{2N_{SW}^2}{\pi k_{SW}} \cdot \frac{\beta_{gr}\lambda}{\sin\theta} \approx 12\ \text{m}, \tag{3.3}$$

which is much longer than current technological limitations.

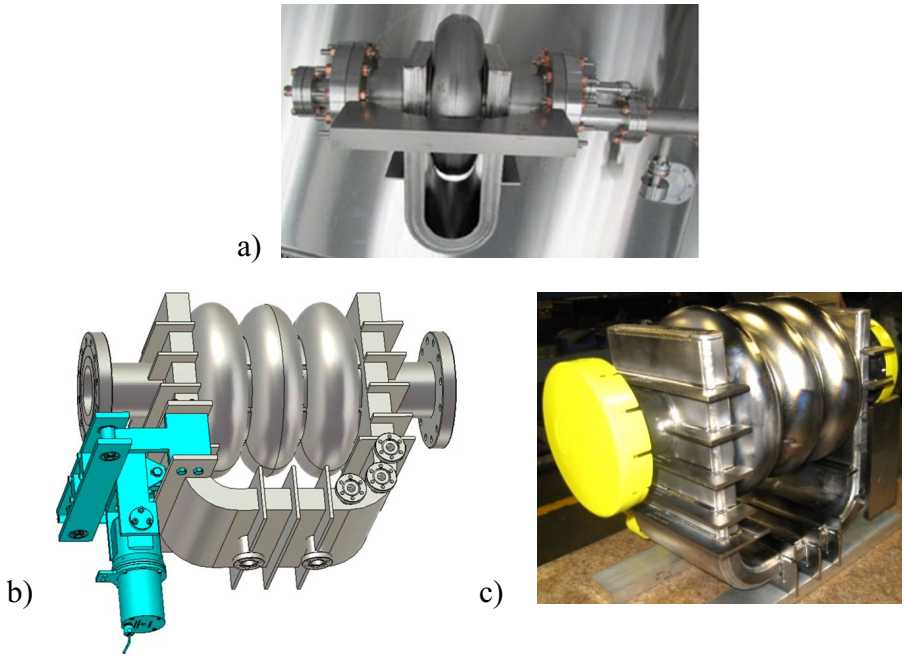

Figure 10. (a) Single-cell TW niobium structure with feedback waveguide, treated by BCP and tested to reach 26 MV/m; (b) 3D model of the 3-cell TW structure; (c) Fabricated 3-cell cavity.

Many significant challenges must still be addressed along the TW development path. High circulating power in the feedback waveguide must be demonstrated. Cavity fabrication and surface processing procedures and fixtures must deal with (roughly) double the number of cells per structure.

First structure fabrication and testing efforts have started for TW cavity development [32]. With the relatively easier BCP treatment only, the first single-cell TW cavity (Figure 10(a)) with recirculating waveguide achieved 26 MV/m accelerating gradient, limited by the high field Q-slope, as expected for BCP. This result is very encouraging for the first attempt. A 3-cell Nb TW structure with recirculating waveguide, shown in Figure 10(b, c), was designed, fabricated, tuned, and processed [33, 34] but has not yet been tested.

4 HELEN collider

For more than four decades, efforts have been devoted to developing high-gradient RF technology linear e^+e^- colliders in order to overcome the synchrotron radiation limitations of circular e^+e^- machines. In linear colliders, where each bunch collides only once, the primary challenge confronting high luminosity is the beam power requirement [35]:

$$\mathcal{L} = \frac{1}{8\pi\alpha r_0}\,\frac{P_{\rm wall}}{\sqrt{s}}\,\frac{\eta}{\sigma_y^*}\,N_\gamma\,H_{\rm D}\,. \tag{4.1}$$

Here, $P_{\rm wall}$ is the total wall-plug power of the collider, to be converted into beam power $P_{\rm b} = 2f_0NE_{\rm b}$ with efficiency η, $N_\gamma \approx 2\alpha r_0 N/\sigma_x^*$ is the number of beamstrahlung photons emitted per $e^\pm$ (α denotes the fine-structure constant), and the last factor $H_{\rm D}$, typically between 1 and 2, represents the enhancement of luminosity due to the *pinch effect*, the additional focusing occurring during

the collision of oppositely charged bunches. To maximize the luminosity with fixed $P_{\rm wall}$, one has to push the bunch population N and cope with beamstrahlung (radiation of photons due to the electromagnetic field of opposing bunch).

Beamstrahlung is very much an issue for all linear colliders as it may significantly widen the luminosity center of mass energy (c.m.e.) spectrum, especially at higher c.m.e. above ~500 GeV. The effect is mitigated by making the colliding beams as flat as possible at the interaction point ($\sigma_x^* \gg \sigma_y^*$). The photon energy spectrum of the beamstrahlung is characterized by the parameter $\Upsilon = (2/3)\hbar\omega_{\rm c}/E_{\rm b}$ [36], with $\hbar\omega_{\rm c}$ denoting the critical photon energy and $E_{\rm b}$ the beam energy. The spectrum strongly deviates from the classical synchrotron radiation spectrum for Υ approaching or exceeding 1. Keeping a significant fraction of the luminosity close to the nominal energy represents a design goal, which is met if N_γ does not exceed a value of about 1. A consequence is the use of flat beams, where N_γ is managed by the beam width, and luminosity adjusted by the beam height, thus the explicit appearance of the vertical beam size σ_y^*.

The strength of the EM beam-beam interaction at the IP of linear colliders is determined by the *disruption parameter* D_y – the ratio of the rms bunch length σ_z to the beam-beam focal length – related to the beam-beam parameter ξ_y via $D_y = 4\pi\sigma_z\xi_y/\beta_y^*$. Significant disruption leads to effectively smaller beam size due to *traveling focus* effect, and a resulting luminosity enhancement. It also makes the collision more sensitive to small offsets, resulting in a *kink instability*. Additional effects arising include e^+e^- pair creation, and depolarization by various mechanisms.

In Table 2 we compare tentative baseline parameters of HELEN with other e^+e^- linear colliders. For a comprehensive evaluation of future colliders we refer the readers to [37]. As mentioned in section 3.2.2, high stability of field distribution along the TW structure allows for longer structures. For the baseline HELEN parameters we assumed the active cavity length of 2.37 m, about 2 times longer than TESLA cavity. As it is obvious from the table, HELEN is in many aspects a high-gradient modification of the International Linear Collider (ILC). The ILC has a baseline center-of-mass energy of 500 GeV or 250 GeV for a Higgs factory option [10]. The ILC is based on the 1.3 GHz TESLA superconducting accelerating structures with 31.5 MV/m average gradient, and aims at 7.7 nm vertical beam size at the IP. Several scenarios of luminosity and energy upgrades of the ILC are under consideration [10, 21]. In Table 2 we list ILC parameters for the Initial and $\mathcal{L}$ Upgrade Higgs factory from [10] and for the 500 GeV center-of-mass energy from [9]. The ILC luminosity upgrade scenarios are directly applicable to HELEN. Possible energy upgrade options we consider in section 4.2.

CERN's Compact Linear Collider (CLIC) design [38], under development since the mid-1980s, also includes possible upgrades, from an initial 380 GeV c.m.e. to ultimately 3 TeV, which would enable searches for new particles of significantly higher masses. CLIC is based on a novel two-beam acceleration scheme in which normal conducting (NC) copper high-gradient 12 GHz accelerating structures are powered by a high-current 1.9 GeV drive beam to enable accelerating gradients up to 100 MV/m (though optimal gradient for the first CLIC stage at $\sqrt{s}$ = 380 GeV is 70 MV/m, and for this stage an alternative RF power drive option with 12 GHz klystrons powering is also being considered).

Recent "Cool Copper Collider" (C^3) proposal [39] envisions klystron-driven C-band NC cavities operating at liquid nitrogen temperatures to achieve higher shunt impedance, smaller breakdown rate, and 70–120 MV/m accelerating gradients.

All linear colliders have a lot in common, e.g., their main subsystems include damping rings, and sophisticated beam delivery (final focus) systems. To reach their design luminosities, linear colliders require very high rates of positron production, and very tight control of imperfections, such as $O(10\ \mu\text{m})$ accuracy of pre-alignment of the main linac and beam delivery system components, suppression of fast vibrations of the quadrupoles due to ground motion to $O(1$ nm) level at frequencies above 1 Hz, advanced beam-based trajectory tuning, and mitigation of wakefield effects.

The traveling wave SRF provides an optimal combination of the high accelerating gradient of 70 MV/m with an expected demonstration of a fully developed cryomodule within $\sim$ 5 – 10 years, providing that sufficient funding is available. It is the most efficient in terms of AC power consumption and is on par with the ILC site power demand. It offers significant cost saving. Our preliminary estimate indicates that the cost savings (relative to the ILC main linac cost) are about 37%.

4.1 Emittance preservation and luminosity degradation control

Main sources leading to emittance growth and/or luminosity degradation in linear colliders are: a) wakefield effects, primarily in accelerating RF structures but also from other apertures such as collimators; b) chromatic (i.e., dispersive) effects, arising from magnet misalignment and beam trajectory errors; and c) beam-beam separation at the IP due to jitter of the final focus quadrupoles.

HELEN, as the ILC, has quite relaxed (compared to other linear collider proposals) alignment and jitter tolerances due to two factors: a) large aperture L-band superconducting RF cavities having the relatively low cavity wakefields and mechanically alignment accuracy of the accelerating cavities $O(300\ \mu\text{m})$ is good enough for suppressing single-bunch wakefield effect to acceptable levels; and b) long pulse train and significant bunch spacing that allows to measure position of the first few bunches and apply necessary corrections to keep the rest of the train on right trajectory. Beam Position Monitors (BPMs) accuracy $O(1\ \mu\text{m})$ is typically sufficient for the beam-based feedback system that includes: a) a slow feedback correcting the beam orbit to compensate for low frequency ground motion; b) an inter-pulse feedback acting in a few locations to correct accumulated errors that occur in between the action of the slow system and to provide the possibility of straightening the beam; and c) a fast intra-train feedback system acting at the IP to keep the beams in collision, correcting for the high frequency ground motion that moves the final quadrupole doublet. Fermilab has significant expertise in the area of collider element stabilization and emittance control, and several important experimental studies indicate that Fermilab's site is sufficiently quiet for an L-band linear collider [40, 41].

4.2 Layout, siting, and upgrades

The layout of the collider (Figure 11) is similar to that of the ILC. We assumed the length occupied by the beam delivery system (BDS) to be 3 km. With the accelerating structures about 2 times longer than TESLA cavities, the fill factor of HELEN SRF linac increases to 80.4% and the collider will be 7.5 km long. As it is discussed in [42], there are three possible locations for a linear collider at Fermilab: two 7-km NE–SW orientations fitting diagonally on the site (Figure 3 in [42]), and a 12-km footprint with N–S orientation extending outside Fermilab boundary, but with the

Parameter	HELEN	C^3	ILC (Initial, $\mathcal{L}$ Upgrade, 500)	CLIC
CM energy $2\times E_b$ (GeV)	250, 500	250, 550	250, 250, 500	380, 3000
Length (km)	7.5, 11.9	8, 8	20.5, 20.5, 31	11.4, 50
Interaction points	1	1	1	1
Integrated luminosity (ab^{-1}/yr)	0.2, 0.3	0.2, 0.4	0.2, 0.4, 0.3	0.1, 0.6
Peak lumi. $\mathcal{L}$ ($10^{34} cm^{-2} s^{-1}$)	1.35, 1.8	1.3, 2.4	1.35, 2.7, 1.8	1.5, 6
CM energy spread ~ $0.4\delta_{BS}$ (rms, %)	1, 1.7	1.6, 7.6	1, 1, 1.7	1.7, 5
Polarization (%)	80/30 (e^-/e^+)	80/0 (e^-/e^+)	80/30 (e^-/e^+)	80/0 (e^-/e^+)
Repetition rate f_{rep} (Hz)	5	120	5	50
Bunch spacing (ns)	554	5.26, 3.5	554, 355, 554	0.5
Particles per bunch N (10^{10})	2	0.63	2	0.52, 0.37
Bunches per pulse n_b	1312	133, 75	1312, 2625, 1312	352, 312
Pulse duration (μs)	727	0.7, 0.26	727, 961, 727	0.176, 0.156
Pulsed beam current I_b (mA)	5.8	190, 286	5.8, 8.8, 5.8	1670, 1190
Bunch length σ_z (rms, mm)	0.3	0.1	0.3	0.07, 0.044
IP beam size σ^* (rms, μm)	H: 0.516, 0.474 V: 0.0077, 0.0059	H: 0.23, 0.16 V: 0.004, 0.0026	H: 0.516, 0.516, 0.474 V: 0.0077, 0.0077, 0.0059	H: 0.15, 0.04 V: 0.003, 0.001
Emittance, ε_n (rms, μm)	H: 5 V: 0.035	H: 0.9 V: 0.02	H: 5 V: 0.035	H: 0.95, 0.66 V: 0.03, 0.02
β^* at interaction point (mm)	H: 13, 11 V: 0.41, 0.48	H: 12 V: 0.12	H: 13, 13, 11 V: 0.41, 0.41, 0.48	H: 8, 6.9 V: 0.1, 0.068
Full crossing angle θ_c (mrad)	14	14	14	20
Crossing scheme	crab crossing	crab crossing	crab crossing	crab crossing
Disruption parameter D_y	35, 25	12	35, 35, 25	13, 8
RF frequency f_{RF} (MHz)	1300	5712	1300	11994
Accelerating gradient E_{acc} (MV/m)	70	70, 120	31.5	72, 100
Effective gradient E_{eff} (MV/m)	55.6	63, 108	21	57, 79
Total beam power (MW)	5.3, 10.5	4, 4.9	5.3, 10.5, 10.5	5.6, 28
Site power (MW)	110, ~190	~150, ~175	111, 136, 173	168, 590
Key technology	TW SRF	cold NC RF	SW SRF	two-beam accel.

Table 2. Tentative parameters of HELEN and other e^+e^- linear collider Higgs factory proposals. Parameters associated with different beam energy scenarios are comma-separated; H and V indicate horizontal and vertical directions; a fill factor of 80.4% is assumed to calculate the real-estate (effective) gradient E_{eff} of HELEN.

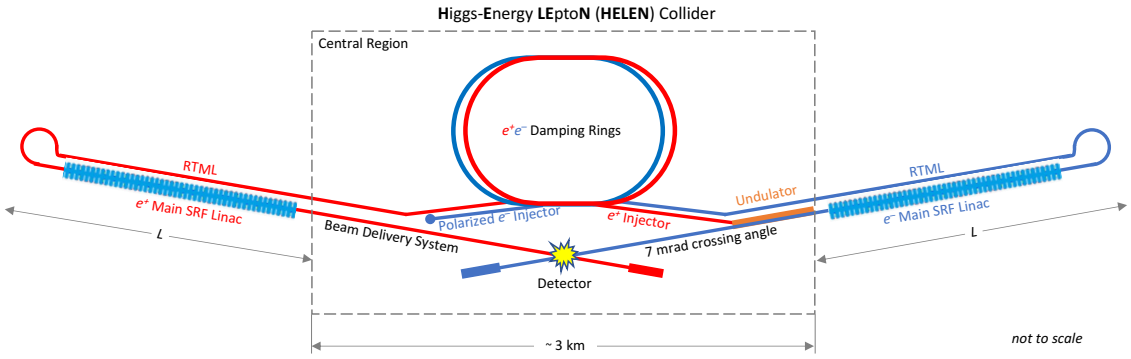

Figure 11. Conceptual layout of the HELEN collider.

Interaction Region (IR) remaining on site. Figure 12 show three possible sitings of HELEN collider on Fermilab site for the 250 GeV c.m.e. As HELEN is similar to ILC in many respects, all proposed ILC luminosity upgrade scenarios (see, e.g., [10]) are applicable. A possible energy upgrades up to 500 GeV, would fill the entire 12 km N-S footprint (see Figure 13).

5 Detector for HELEN Collider

A possible detector for the HELEN collider could look very similar to proposed detector concepts for the ILC [43] or CLIC [4, 44] and would profit immensely from previous studies and R&D carried out by those communities. Detailed simulation studies would of course have to be carried out, but by first principles we can assume that the fundamental challenges and requirements would be similar. The physics program determines the detector requirements with some of the key points being high-resolution jet energy reconstruction and di-jet mass resolution to separate W and Z di-jet final states; excellent momentum resolution for charged particles driven by the need to reconstruct the Higgs boson recoiling from leptonically decaying Z bosons; and unprecedented flavor tagging.

In general such a detector would call for a highly-efficient, very low-mass, small-pixel vertexing and tracking system enabling good flavor tagging and heavy and light quark separation, as well as excellent transverse momentum resolution for high-p_T tracks. The latter also requires a large magnetic field on the order of 4 T surrounding the tracking and calorimeter systems. The concept of pulsed power applications, as well as ultra-lightweight cooling and support structures need to be considered in order to keep the overall detector mass in the innermost region at the lowest possible level. In order to enable unprecedented energy resolution, high-granularity electromagnetic and hadronic calorimeters are needed. Detector coverage for electrons and photons needs to extend to very low polar angles to aid in the rejection of large background levels from beamstrahlung. Also for the calorimeters pulsed power readout electronics would be beneficial, taking advantage of the low-duty cycle beam structure of a linear collider, and allowing to forego the need for active cooling. Muon identification would be performed by an instrumented iron return yoke on the outside of the detector. Precision timing on the order of ns might be important for background tagging and pileup rejection, but should be less relevant than for example for CLIC, given the much longer bunch trains, and longer gaps. Radiation hardness is much less a concern than for current LHC experiments, as

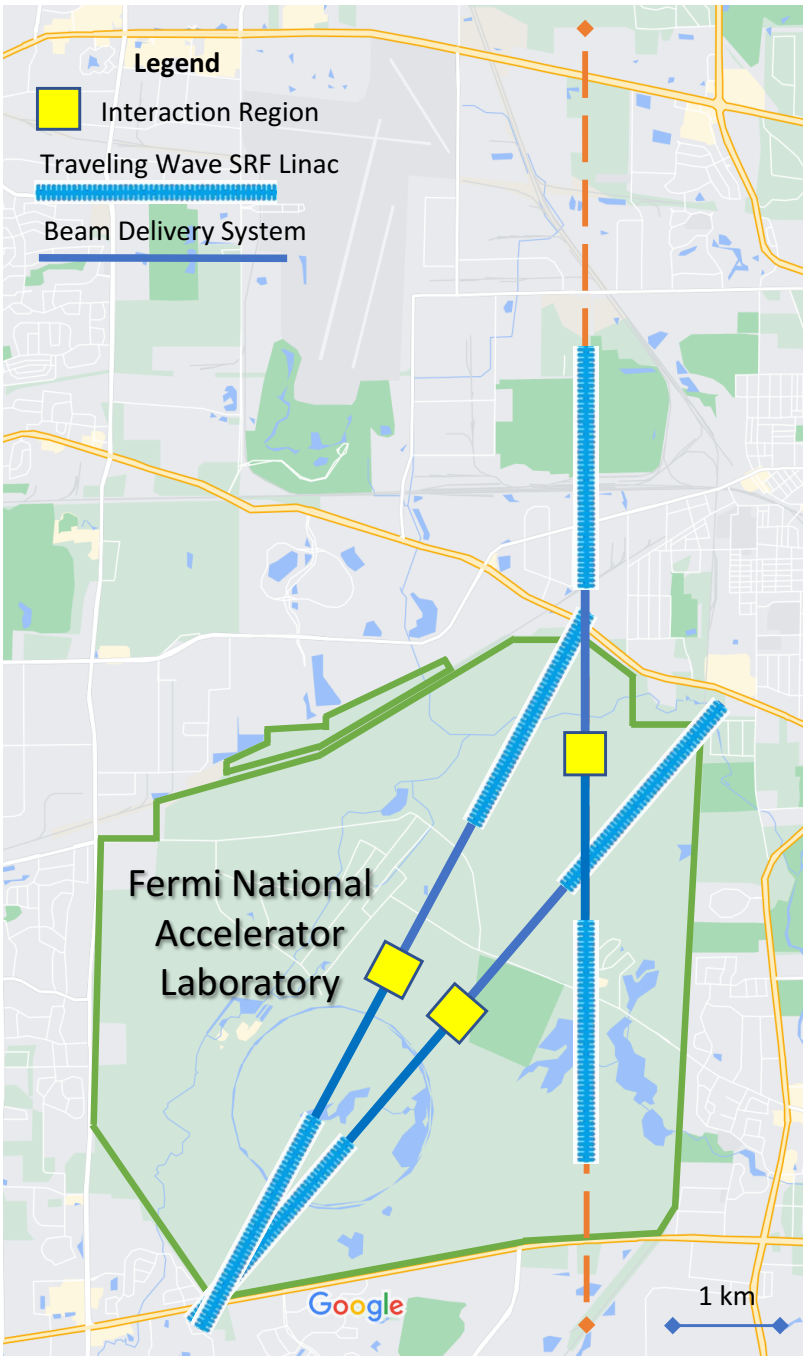

Figure 12. Three possible sitings of 250 GeV c.m.e. HELEN collider at Fermilab. The orange dashed line indicates a 12-km stretch that might be made available for a future linear collider.

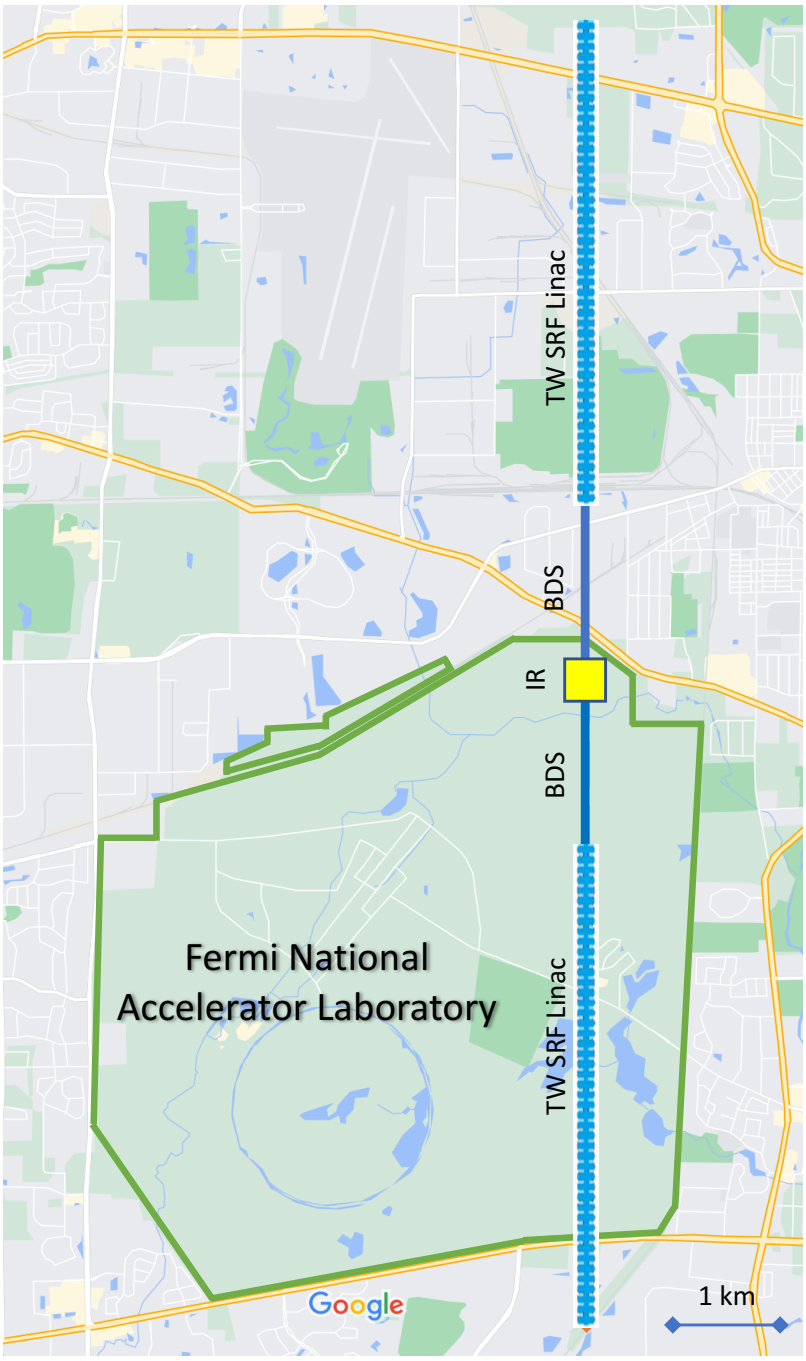

Figure 13. 500 GeV HELEN collider at Fermilab.

the expected TID and NIEL levels are going to be orders of magnitude lower. Concerning the data volume and rates, even with continuous, triggerless readout they should be well below current LHC readout rates.

Fermilab provides a range of detector facilities and technical capabilities that could aid the development of several of these detector components. With SiDet we have a world-class silicon micro- and macro-packaging facility, which has been originally built for the development and construction of the silicon detectors for the Tevatron experiments D0 and CDF. Since then we have built many generations of state-of-the-art semiconductor detectors for collider experiments and astro-particle physics there. We have a large group of ASIC designers in house, who have collaborated on many key chips for HEP experiments. With our scintillator facility we have contributed extruded scintillator to many HEP efforts, as well as performed R&D into molded and 3D-printed scintillators. The on-site testbeam and irradiation facilities complement the technological expertise.

6 Accelerator and detector R&D for HELEN collider

6.1 Accelerator R&D program objectives

The major objectives of the accelerator R&D program are on advancing the TW SRF technology toward demonstrating its feasibility, should be accompanied by a few other important items, and culminate in producing a Technical Design Report:

- Demonstrate the feasibility of the TW SRF technology:
  - test proof-of-principle 1.3 GHz TW cavity (0.5 to 1 meter long structure) and demonstrate accelerating gradient of $\sim$ 70 MV/m
  - adapt an advanced cavity treatment techniques, so that high $Q \sim 10^{10}$ can be achieved at high gradients
  - design, build and test full-scale prototype cavities; demonstrate performance needed for the HELEN collider
  - design and build a cryomodule for TW SRF cavities
  - verify the cryomodule performance without beam on a test stand and with beam at Fermilab's FAST facility
- Design and optimize the HELEN linear collider accelerator complex
- Confirm the physics reach and detector performance for the HELEN beam parameters
- Publish a Conceptual Design Report as modification of the ILC design in $\sim$ 5 years
- Prepare a Technical Design Report after demonstrating the cryomodule performance

6.2 Detector R&D program objectives

Given that funding for generic, "blue sky" R&D is scarce, the most practical approach to solving some of the technological limitations for future collider detectors is to identify appropriate intermediate projects (e.g., future LHCb and ALICE upgrades, EIC, etc.) that could serve as stepping

stones, or small- to mid-scale technology demonstrators. For example for the inner vertexing detector, R&D on various technologies is already going on, with advances in CMOS detectors taking most of the recent focus. Especially recent developments by Mu3e [45] and ALICE [46] into ultra-lightweight support structures made of Kapton, or wafer-sized, bent sensors, are of strong relevance here. Furthermore, R&D into novel, room-temperature refrigerants, air cooling, silicon micro-channel cooling directly etched into the silicon sensor's backside, or carbon-based cooling pipes lay out promising R&D directions.

For the highly-granular calorimeters, which are essential to support necessary particle flow algorithms, several technologies are being investigated. Many of which have been demonstrated over many years within the CALICE collaboration [47]. One specific application is currently being built within the context of the HL-LHC CMS Detector Upgrade. The main challenges here are the overall size, complexity and cost of the detector. Some of the technology choices available are silicon as sensitive material, liquid argon calorimetry, or dual readout calorimeters containing fibers or crystals. Each of these has advantages and disadvantages related to energy resolution, containment and granularity. One particular recent interest that has emerged is the addition of fast timing information within the calorimeter, where 20–50 ps timing resolution per hit would enable 5D calorimetry and thus tracking inside showers. R&D needs to be performed on LGAD sensors to optimize sensors thickness with regard to signal size and timing resolution.

There are strong R&D plans for ILC, FCC and other e^+e^- factories planned which are fully applicable to the HELEN main detector requirements on tracking, calorimeter, readout, etc.

7 Summary and conclusions

In this paper we presented a proposal for a Higgs factory based on traveling wave SRF technology. Recent achievements and anticipated near-future progress in this technology allow us to consider a linear e^+e^- collider with an accelerating gradient of ~ 70 MV/m. The HELEN collider resembles the ILC in many aspects and would offer a similar physics program. The benefits of the HELEN collider are twofold: i) it offers an estimated 37% main linac cost saving with respect to the ILC main linac and ii) due to higher accelerating gradient, the collider's smaller footprint could potentially be implemented at Fermilab.

Dedicated R&D efforts are still necessary to make further advances and demonstrate feasibility of the proposed approach. However, with an appropriate level of new investment this focused program could be accomplished in $\sim 5-10$ years, after which a Technical Design Report would be prepared. This program would be a part of the integrated U.S. collider R&D program proposed in [42].

Acknowledgments

This work was produced by Fermi Research Alliance, LLC under Contract No. DE-AC02-07CH11359 with the U.S. Department of Energy. Publisher acknowledges the U.S. Government license to provide public access under the DOE Public Access Plan (http://energy.gov/downloads/doe-public-access-plan).

References

[1] Belomestnykh et al., "Higgs-energy lepton (helen) collider based on advanced superconducting radio frequency technology." https://arxiv.org/abs/2203.08211, 2022.

[2] "The International Linear Collider Technical Design Report – Volume 2: Physics." https://arxiv.org/abs/1306.6352, June, 2013.

[3] FCC collaboration, *FCC Physics Opportunities: Future Circular Collider Conceptual Design Report Volume 1*, *Eur. Phys. J. C* **79** (2019) 474.

[4] "Physics and Detectors at CLIC: CLIC Conceptual Design Report." CERN-2012-003, ANL-HEP-TR-12-01, DESY-12-008, KEK-REPORT-2011-7, https://arxiv.org/abs/1202.5940, February, 2012.

[5] M. Ahmad et al., *CEPC-SPPC Preliminary Conceptual Design Report. Volume 1. Physics and Detector*, Tech. Rep. IHEP-CEPC-DR-2015-01, IHEP-TH-2015-01, IHEP-EP-2015-01 (March, 2015).

[6] S. Dawson et al., *Working Group Report: Higgs Boson*, in *Community Summer Study 2013: Snowmass on the Mississippi*, October, 2013, https://arxiv.org/abs/1310.8361.

[7] *Proceedings of the 1st TESLA (TeV Superconducting Linear Accelerator) Workshop*, no. CLNS 90-1029, (Cornell University, Ithaca, NY, USA), 1990.

[8] C. Adolphsen, M. Barone, B. Barish, K. Buesser, P. Burrows, J. Carwardine et al., "The International Linear Collider Technical Design Report – Volume 3.I: Accelerator R&D in the Technical Design Phase." https://arxiv.org/abs/1306.6353, 2013.

[9] C. Adolphsen, M. Barone, B. Barish, K. Buesser, P. Burrows, J. Carwardine et al., "The International Linear Collider Technical Design Report – Volume 3.II: Accelerator Baseline Design." https://arxiv.org/abs/1306.6328, 2013.

[10] The ILC International Development Team and the ILC community, "The International Linear Collider: Report to Snowmass 2021." https://arxiv.org/abs/2203.07622, 2022.

[11] H. Padamsee, A. Grassellino, S. Belomestnykh and S. Posen, "Impact of high Q on ILC250 upgrade for record luminosities and path toward ILC380." https://arxiv.org/abs/1910.01276, 2019.

[12] B. Aune et al., *Superconducting TESLA cavities*, *Phys. Rev. Accel. Beams* **3** (2000) 092001.

[13] "The European X-Ray Free-Electron Laser: Technical Design Report." https://bib-pubdb1.desy.de/record/77248/files/european-xfel-tdr.pdf, July, 2007.

[14] T. O. Raubenheimer for the LCLS-II Collaboration, *Technical Challenges of the LCLS-II CW X-ray FEL*, in *Proceedings of the 6th Int. Particle Accel. Conf. IPAC2015*, (Richmond, VA, USA), pp. 2434–2438, JACoW Publishing, 2015, http://dx.doi.org/10.18429/JACoW-IPAC2015-WEYC1.

[15] D. Reschke, S. Aderhold, A. Goessel, J. Iversen, S. Karstensen, D. Kostin et al., *Results on large grain nine-cell cavities at DESY: gradients up to 45 MV/m after electropolishing*, in *Proceedings of SRF2011*, (Chicago, IL, USA), pp. 490–494, 2011.

[16] M. Pekeler, "Superconducting RF cavity system production for particle accelerators in scientific and industrial applications." presentation at the 38th Int. Conf. on High Energy Phys., ICHEP2016, August, 2016.

[17] K. Kasprzak, M. Wiencek, A. Zwozniak, D. Kostin, D. Reschke and N. Walker, *Test results of the European XFEL serial-production accelerator modules*, in *Proceedings of the 18th Int. Conf. on RF Supercond.*, (Lanzhou, China), pp. 312–316, JACoW Publishing, 2017, http://dx.doi.org/10.18429/JACoW-SRF2017-MOPB106.

[18] C. Schmidt, J. Branlard, M. Bousonville, M. Diomede, S. Göller, D. Kostin et al., *Operational experience with the European XFEL SRF linac*, in *Proceedings of the 21st Int. Conf. on RF Supercond.*, (Grand Rapids, MI, USA), JACoW Publishing, 2023.

[19] D. Broemmelsiek, B. Chase, D. Edstrom, E. Harms, J. Leibfritz, S. Nagaitsev et al., *Record high-gradient SRF beam acceleration at Fermilab*, *New J. Phys.* **20** (2018) 113018.

[20] Y. Yamamoto et al., *Stable beam operation at 33 MV/m in STF-2 cryomodules at KEK*, in *Proceedings of SRF2021*, (East Lansing, MI, USA), 2021.

[21] H. Padamsee, "ILC upgrades to 3 TeV." https://arxiv.org/abs/2108.11904, 2021.

[22] A. Grassellino, A. Romanenko, D. Sergatskov, O. Melnychuk, Y. Trenikhina, A. Crawford, A. Rowe, M. Wong, T. Khabiboulline and F. Barkov, *Nitrogen and argon doping of niobium for superconducting radio frequency cavities: a pathway to highly efficient accelerating structures*, *Supercond. Sci. Technol.* **26** (2013) 102001.

[23] D. Gonnella for the LCLS-II-HE Collaboration, "LCLS-II-HE High Q_0 & Gradient R&D Program, First CM Test Results, and CM Plasma Processing Results." presentation at the virtual TESLA Technology Collaboration Meeting, January, 2022.

[24] S. Posen, A. Romanenko, A. Grassellino, O. S. Melnychuk and D. A. Sergatskov, *Ultralow surface resistance via vacuum heat treatment of superconducting radio-frequency cavities*, *Phys. Rev. Applied* **13** (2020) 014024.

[25] F. He, W. Pan, P. Sha, J. Zhai, Z. Mi, X. Dai et al., "Medium-temperature furnace bake of superconducting radio-frequency cavities at IHEP." https://arxiv.org/abs/2012.04817, 2020.

[26] A. Grassellino, A. Romanenko, Y. Trenikhina, M. Checchin, M. Martinello, O.S. Melnychuk et al., *Unprecedented quality factors at accelerating gradients up to 45 MVm^{-1} in niobium superconducting resonators via low temperature nitrogen infusion*, *Supercond. Sci. Technol.* **30** (2017) 094004.

[27] A. Grassellino, A. Romanenko, D. Bice, O. Melnychuk, A.C. Crawford, S. Chandrasekaran et al., "Accelerating fields up to 49 MV/m in TESLA-shape superconducting RF niobium cavities via 75C vacuum bake." https://arxiv.org/abs/1806.09824, 2018.

[28] D. Bafia, A. Grassellino, Z. Sung, A. Romanenko, O.S. Melnychuk and J.F. Zasadzinski, *Gradients of 50MV/m in TESLA shaped cavities via modified low temperature bake*, in *Proceedings of 19th Int. Conf. on RF Superconductivity SRF2019*, (Dresden, Germany), pp. 586–591, JACoW Publishing, 2019, http://dx.doi.org/10.18429/JACoW-SRF2019-TUP061.

[29] R.B. Neal, *Consideration of the use of feedback in a traveling wave superconducting accelerator*, Tech. Rep. SLAC-PUB-437 (June, 1968).

[30] V. Yakovlev et al., *Excitation of a traveling wave in a superconducting structure with feedback*, in *Proceedings of 23rd Particle Accel. Conf. PAC2009*, (Vancouver, BC, Canada), pp. 969–971, 2009, https://accelconf.web.cern.ch/PAC2009/papers/tu5pfp062.pdf.

[31] V. Shemelin, H. Padamsee and V. Yakovlev, *Optimization of a traveling wave superconducting rf cavity for upgrading the International Linear Collider*, *Phys. Rev. Accel. Beams* **25** (2022) 021001.

[32] R. Kostin, P. Avrakhov, A. Kanareykin, N. Solyak, V. Yakovlev, S. Kazakov et al., *A high gradient test of a single-cell superconductivity at radio frequency cavity with a feedback waveguide*, *Supercond. Sci. Technol.* **28** (2015) 095007.

[33] R. Kostin, P. Avrakhov, A. Kanareykin, V. Yakovlev and N. Solyak, *Progress towards 3-cell superconducting traveling wave cavity cryogenic test*, *J. Phys.: Conf. Ser.* **941** (2017) 012100.

[34] F. Furuta, V. Yakovlev, T. Khabiboulline, R. Kostin and P. Avrakhov, *Development of 3-cell traveling wave SRF cavity*, in *Proceedings of 21st Int. Conf. on RF Supercond. SRF2023*, (Grand Rapids, MI, USA), JACoW Publishing, 2023.

[35] V. Shiltsev and F. Zimmermann, *Modern and future colliders*, *Rev. Mod. Phys.* **93** (2021) 015006.

[36] K. Yokoya and P. Chen, *Beam-beam phenomena in linear colliders*, in *Frontiers of Particle Beams: Intensity Limitations*, M. Dienes, M. Month and S. Turner, eds., (Berlin, Heidelberg), pp. 415–445, Springer, 1992, DOI.

[37] T. Roser, R. Brinkmann, S. Cousineau, D. Denisov, S. Gessner, S. Gourlay et al., *On the feasibility of future colliders: report of the Snowmass'21 Implemetation Task Force*, *JINST* **18** (2023) P05018.

[38] "The Compact Linear Collider (CLIC) – Project Implementation Plan." https://arxiv.org/abs/1903.08655, 2019.

[39] M. Bai, T. Barklow, R. Bartoldus, M. Breidenbach, P. Grenier, Z. Huang et al., "C^3: A "Cool" Route to the Higgs Boson and Beyond." https://arxiv.org/abs/2110.15800, 2021.

[40] B. Baklakov, T. Bolshakov, A. Chupyra, A. Erokhin, P. Lebedev, V. Parkhomchuk et al., *Ground vibration measurements for Fermilab future collider projects*, *Phys. Rev. Accel. Beams* **1** (1998) 031001.

[41] V. Shiltsev, *Review of observations of ground diffusion in space and in time and fractal model of ground motion*, *Phys. Rev. Accel. Beams* **13** (2010) 094801.

[42] P.C. Bhat, S. Jindariani, G. Ambrosio, G. Apollinari, S. Belomestnykh, A. Bross et al., "Future Collider Options for the US." https://arxiv.org/abs/2203.08088, 2022.

[43] T. Behnke, J.E. Brau, P.N. Burrows, J. Fuster, M. Peskin, M. Stanitzki et al., "The International Linear Collider Technical Design Report - Volume 4: Detectors." https://arxiv.org/abs/1306.6329, 2013.

[44] CLICdp collaboration, D. Dannheim et al., *Detector technologies for CLIC*, CERN Yellow Reports: Monographs (May, 2019), 10.23731/CYRM-2019-001.

[45] Mu3e collaboration, *Technical design of the phase I Mu3e experiment*, *Nucl. Instrum. Methods Phys. Res., Sect. A* **1014** (2021) 165679.

[46] Felix Reidt (on nehalf of the ALICE collaboration), "Upgrade of the ALICE ITS detector." https://arxiv.org/abs/2111.08301, 2022.

[47] "The CALICE Collaboration." https://twiki.cern.ch/twiki/bin/view/CALICE/WebHome.